

# Absorption and emission spectra of a Schwarzschild black hole

Norma Sanchez

*Département d'Astrophysique Fondamentale, Observatoire de Paris 92190, Meudon, France*

(Received 8 March 1977)

The absorption spectrum of a Schwarzschild black hole is studied in detail. Accurate and useful computational methods based on the analytical resolution of the wave equation are developed. In this way phase shifts and absorption cross sections are obtained for a wide range of energy and angular momentum. Comparison with the explicit results valid for low and high frequencies is made. The total absorption cross section of the black hole is obtained as a function of the energy. It presents behavior characteristic of a diffraction pattern. The constant geometric-optics limit  $[(27/4)\pi r_s^2]$  is approached in an oscillatory fashion. The physical interpretation of these results is given and a simple model which describes qualitatively the absorption of waves by the black hole is presented. From these absorption parameters, the Hawking emission rates are calculated and their properties discussed.

## I. INTRODUCTION

In the context of classical field theory, black holes absorb waves but they cannot emit them. However, if quantum effects are considered the energy emitted in each mode of frequency  $k$  and angular momentum  $l$  is given by Hawking's formula<sup>1</sup>

$$dH_l(k) = \frac{\mathcal{P}_l(k)}{e^{4\pi k r_s} - 1} \frac{2l+1}{\pi} k dk \quad (1)$$

(where  $r_s = 2M$ , with  $M$  the mass of the hole).

Qualitative aspects and rough order-of-magnitude estimates of Hawking emission have been discussed by Carter<sup>2</sup> and many subsequent authors (see, e.g., DeWitt<sup>3</sup> and references contained therein).

We see that the absorption coefficient  $\mathcal{P}_l(k)$  is an essential parameter in this emission probability. The first attempt to calculate analytical absorption coefficients was made by Starobinsky<sup>4</sup> in the low-energy limit. Numerical calculations have recently been carried out by Page,<sup>5</sup> who calculated total emission rates for the known massless particles. However, the absorption spectrum has not been analyzed in detail up to now.

The present work is a step in the development of more exact and simpler computational methods based on the analytical resolution of the wave equation. Analytical expressions for the absorption (and scattering) parameters for high energy have been reported previously by the present author,<sup>6</sup> namely

$$\mathcal{P}_l(k) = \frac{1 - e^{-4\pi k r_s}}{1 + e^{-4\pi k r_s}} \quad \text{for } l \ll k r_s \gg 1 \quad (2)$$

and

$$\mathcal{P}_l(k) = \frac{1}{1 + \exp\{[(2l+1)\pi][1 - 27k^2 r_s^2/(2l+1)^2]\}} \quad \text{for } l \gg 1, \quad k r_s \gg 1. \quad (3)$$

From these results, it follows that the emission rates  $H_l(k)$  can be expressed very simply by

$$dH_l(k) = \frac{1}{e^{4\pi k r_s} + 1} \frac{2l+1}{2\pi} k dk \quad \text{for } l \ll k r_s \gg 1 \quad (4)$$

and by

$$dH_l(k) = \frac{(2l+1)k dk}{(e^{4\pi k r_s} - 1)\{1 + \exp[(2l+1)\pi(1 - 27k^2 r_s^2/(2l+1)^2)]\}} \quad \text{for } l \gg 1, \quad k r_s \gg 1. \quad (5)$$

In an earlier paper,<sup>7</sup> the formal scattering theory was extended to the black-hole case, allowing a better insight into the theoretical features of the absorption problem. In the present paper we go on to calculate the absorption parameters for a massless scalar field in Schwarzschild geometry, from the exact analytic solutions of the radial equation.

Analytical expressions for the radial solutions defined by power convergent series expansions about  $r = r_s$  and asymptotic power series about  $r = \infty$  have been given by Persides.<sup>8</sup> However, the domains of convergence cover disjoint regions of the  $r$  plane. We have analytically continued the power-series expansions away from their convergence circles in order to calculate them in a common domain (see the Appendix).

The scattering parameters for an incident plane wave have been expressed in terms of the radial solutions via the Jost functions for our problem (Sec. II). In this way, phase shifts and partial absorption amplitudes are obtained for a wide range of energy and angular momentum. This calculation allows us to obtain in detail the total absorption spectrum of the black hole.

In Sec. III, the properties of the imaginary parts of the phase shifts (Fig. 1) and the partial absorption cross sections (Fig. 2) are discussed. The

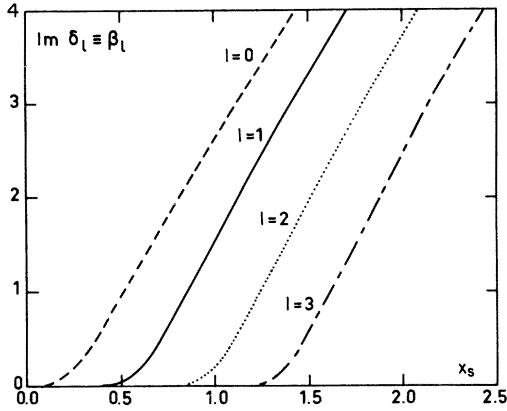


FIG. 1. Imaginary part of the phase shift for  $l=0, 1, 2, 3$ .

results found are compared with the analytical results valid for small<sup>4</sup> and high<sup>6</sup> energies.

All partial absorption amplitudes present absolute maxima around the frequency  $k = \frac{3}{2}(\sqrt{3}/r_s) \times (l + \frac{1}{2})$ , which corresponds to the critical impact parameter given by geometrical optics.<sup>9</sup>

The zero-frequency behavior is analyzed and related to the presence of an  $l$ -order pole in the Jost functions at  $k=0$ . Summing up the contributions of all significant partial waves for each value of the energy, the total absorption cross section

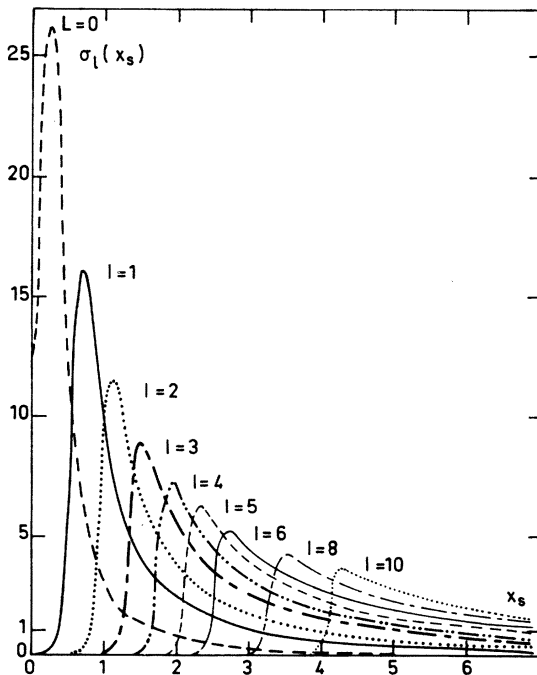


FIG. 2. Partial absorption cross sections  $\sigma_l(x_s)$  in units of  $r_s^2$ .

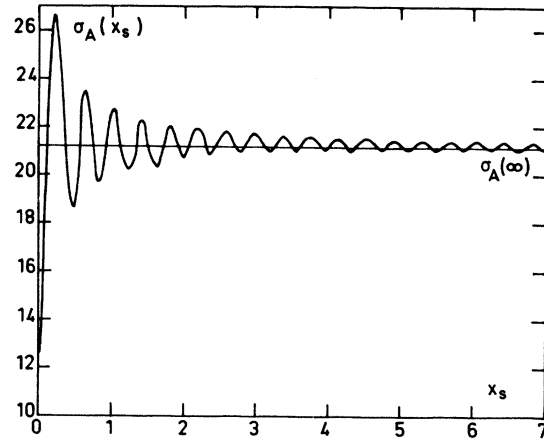


FIG. 3. Total absorption cross section  $\sigma_A(x_s)$  in units of  $r_s^2$  for a Schwarzschild black hole.

( $\sigma_A$ ) is obtained (Fig. 3). The absolute maximum of each partial absorption cross section produces a relative maximum in the total spectrum which presents an oscillatory behavior characteristic of a diffraction pattern. As the frequency increases,  $\sigma_A$  approaches its constant geometric-optics value ( $\frac{27}{4}\pi r_s^2$ ) in an oscillatory way. The period of the oscillations is approximately constant and equal to 0.38, whereas the amplitude decreases with the energy as  $\sqrt{2}/x_s$ .

In a previous paper,<sup>7</sup> we have shown that absorption may be interpreted as taking place only at the singularity ( $r=0$ ) of the Schwarzschild space. Combining these results with the Fresnel-Kirchoff diffraction theory, we show in Sec. III that the oscillatory behavior can be approximated by a simple model in which interference takes place between rays arriving at the origin by different optical paths.

In Sec. III, we also discuss the comparison of the results with the corresponding formulas for absorption by an ordinary material sphere with a complex refractive index, whose total absorption cross section is a monotonically increasing function of frequency (Fig. 4). Comparison with the

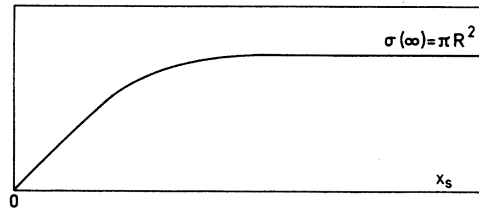


FIG. 4. Total absorption cross section for a material sphere with a complex refractive index. It can be noted that this absorption cross section attains its geometrical-optics limit ( $\pi R^2$ ) without any oscillations.

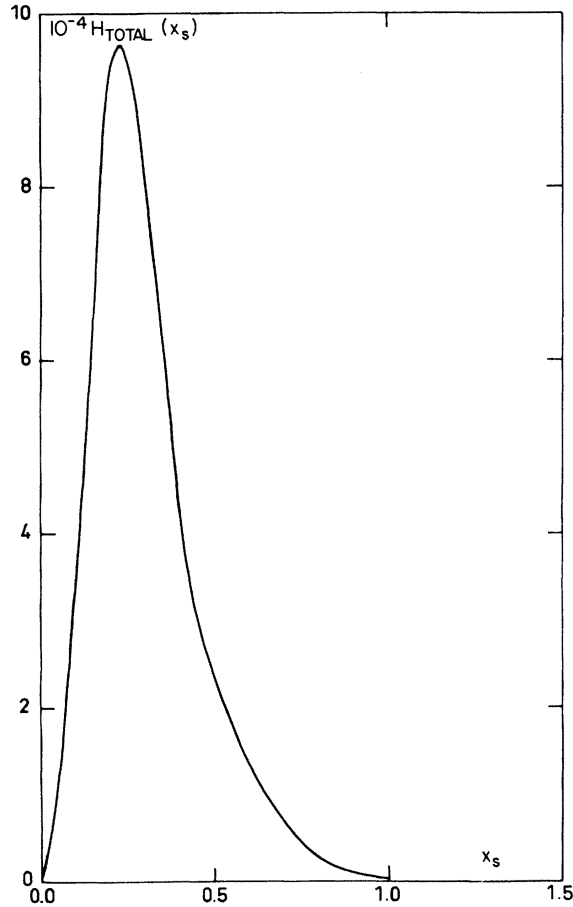


FIG. 5. Total emission spectrum for a black hole in units of  $1/r_s^2$ .

oscillatory black-hole cross section (Fig. 3) shows clearly the differences between the absorptive properties of a black hole and the absorptive properties of a material optical absorber. For a black hole, the presence of a nonzero absorption cross section is related to the non-Hermiticity of the effective potential that describes the wave-black-hole interaction.<sup>7</sup> (We recall that the effective potential of the black hole is non-Hermitian due to its singularity at  $r=0$ , despite being real.)

In Sec. IV, we calculate the emission rates for a wide range of energy and angular momentum using the absorption cross section discussed in Sec. III.

The total emission spectrum as a function of the energy (Fig. 5) does not show any of the oscillations characteristic of the total absorption spectrum. This is due to the rapid decreasing of the Planck factor [Eq. (1)] for  $kr_s \gtrsim 1$ , which suppresses the contribution of the partial waves with  $l \geq 1$ . Hawking emission is only significant in the frequency range  $0 \leq k \lesssim 1/r_s$ .

The calculation of the elastic scattering parameters will be the subject of a subsequent publication.

## II. PHYSICAL AND JOST RADIAL SOLUTIONS IN SCHWARZSCHILD GEOMETRY

In Schwarzschild's space-time, the metric tensor is

$$g_{\mu\nu} = \text{diag} \left[ \left(1 - \frac{r_s}{r}\right), -\left(1 - \frac{r_s}{r}\right)^{-1}, -r^2, -r^2 \sin^2 \theta \right],$$

and the scalar wave equation

$$\square \Psi \equiv g^{\mu\nu} \Psi_{;\mu\nu} = 0$$

is separable. If we consider a solution  $\Psi = R_l(r) Y(\theta, \phi) e^{-i\omega t}$ , the radial wave equation for the  $l$ th partial wave has the following form:

$$x(x-x_s)^2 \frac{d^2 R_l}{dr^2} + (x-x_s)(2x-x_s) \frac{dR_l}{dr} + [x^3 - l(l+1)(x-x_s)] R_l = 0, \quad (7)$$

where  $x = kr$ ,  $x_s = kr_s$ , and  $k = \omega$ . This equation has singularities at  $x=0$ ,  $x=x_s$ , and  $x=\infty$ . The points  $x=0$  and  $x=x_s$  are regular in the sense of the theory of second-order differential equations and  $x=\infty$  is an irregular singular point of the equation.

In terms of the variable  $x^*$  defined by

$$x^* = x + x_s \ln \left( \frac{x}{x_s} - 1 \right),$$

Eq. 7 can be written in the Schrödinger form with an effective potential (Fig. 6) given by

$$V_{\text{eff}}(x^*) = \left(1 - \frac{x_s}{x}\right) \left[ \frac{x_s}{x^3} + \frac{l(l+1)}{x^2} \right]. \quad (8)$$

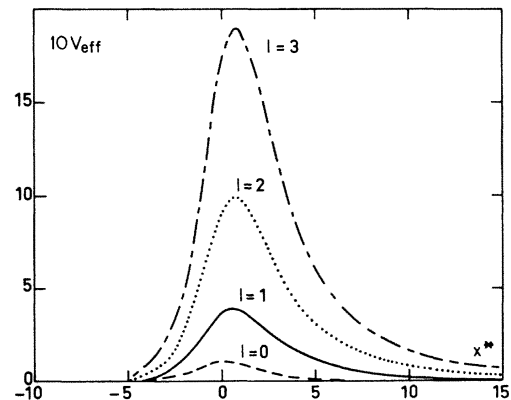


FIG. 6. Effective potential defined by Eq. (8) for  $l=0, 1, 2, 3$ .

Analytical expressions for the radial solution  $R_l(x, x_s)$  defined by power-series expansions about  $x = x_s$  and  $x = \infty$  have been given by Persides.<sup>8</sup> In the neighborhood of  $x = x_s$ , the solution that describes purely ingoing waves on the horizon<sup>8</sup> is

given by

$$R_l(x, x_s) = e^{-ix_s \ln|x-x_s|} \sum_{n=0}^{\infty} d_{ln}(x-x_s)^n, \quad (9)$$

where  $d_{ln}$  satisfies the recurrence relation

$$(n-2ix_s)n x_s d_{ln} + [(n+l)(n-l-1) + 2x_s^2 - (2n-1)ix_s] d_{l, n-1} + 3x_s d_{l, n-2} + d_{l, n-3} = 0. \quad (10)$$

The other linearly independent solution is given by the complex conjugate of Eq. (9).

In the neighborhood of  $r = \infty$ , two linearly independent solutions are

$$\mathcal{F}_{l(\pm)}(x, x_s) = e^{\mp i(x+x_s \ln|x-x_s|)} i^{\pm 1} \sum_{n=0}^{\infty} \tau_{n(\pm)} x^{-(n+1)}, \quad (11)$$

where  $\tau_{n(\pm)}$  satisfies the recurrence relation

$$\pm 2in\tau_{n(\pm)} - (l+n)(l-n+1)\tau_{(n-1)(\pm)} - (n-1)^2 x_s \tau_{(n-2)(\pm)} = 0. \quad (12)$$

The respective functions  $\mathcal{F}_{l(+)}$  ( $\mathcal{F}_{l(-)}$ ) describe purely ingoing (outgoing) waves at infinity and are called the Jost solutions.

In this scattering problem, the physical solution of the wave equation is defined by mixed boundary conditions, one at  $x = x_s$  and one at  $x = \infty$ . One imposes that there are no outgoing waves at  $x = x_s$  (Ref.10) and one fixes the normalization of the ingoing waves, at  $x = \infty$ , by

$$R_l \underset{x \rightarrow \infty}{\sim} i^{l+1} \frac{(2l+1)}{2k} e^{i\delta_l} [e^{-i(x+x_s \ln|x-x_s|)} - (-1)^l S_l(x_s) e^{i(x+x_s \ln|x-x_s|)}] + O\left(\frac{1}{x^2}\right), \quad (13)$$

$$R_l \underset{x \rightarrow x_s}{\sim} g_l(x_s) (x-x_s)^{-ix_s} [1 + O(x-x_s)]. \quad (14)$$

As is well known,  $S_l$  is the partial scattering amplitude connected to the asymptotic behavior of the solution for  $r \rightarrow \infty$ . It can be shown<sup>7</sup> that the coefficient  $g_l \equiv d_{l0}$  connected to the asymptotic behavior near the horizon gives the partial absorption amplitude of waves by the black hole. It is mathematically more convenient to discuss a solution that is defined by boundary conditions at a single point. It is for this reason that one introduces a new radial wave solution  $\varphi_l$ , which differs from the physical solution in its normalization. It is purely ingoing for  $x \rightarrow x_s$  and it is normalized in such a way that

$$\varphi \underset{x \rightarrow x_s}{\sim} (x-x_s)^{-ix_s} [1 + O(x-x_s)]. \quad (15)$$

In order to express the scattering and absorption parameters in terms of the radial solutions it is useful to consider the Jost functions<sup>11</sup> for our problem.

The solutions  $\mathcal{F}_{l(\pm)}$  being linearly independent, the solution  $\varphi_l$  may be written as a linear combination of them:

$$\varphi_l(x, x_s) = f_l^{(-)}(x_s) \mathcal{F}_{l(+)}(x, x_s) + f_l^{(+)}(x_s) \mathcal{F}_{l(-)}(x, x_s). \quad (16)$$

The coefficients  $f_l^{(\pm)}(x_s)$  are called the Jost functions and are given by

$$f_l^{(\pm)}(x_s) = (\pm) \frac{x(x-x_s)}{2i} W[\mathcal{F}_{l(\pm)}(x, x_s), \varphi_l(x, x_s)], \quad (17)$$

where we have used the condition that the Wronskian  $W[\mathcal{F}_{l(+)}, \mathcal{F}_{l(-)}]$  is equal to

$$\frac{2i}{x(x-x_s)}.$$

It follows from Eqs. (11), (17) and the reality of the differential equation that

$$\mathcal{F}_{l(\pm)}^*(x, x_s) = (-1)^{l+1} \mathcal{F}_{l(\mp)}(x, x_s) \quad (18)$$

and

$$f_l^{(\pm)*}(x_s) = (\pm) f_l^{(\pm)}(-x_s) (-1)^l. \quad (19)$$

Comparison of Eq. (16) with the asymptotic behavior of Eq. (13) gives

$$S_l(x_s) \equiv e^{2i\delta_l(x_s)} = - \frac{f_l^{(+)}(x_s)}{f_l^{(-)}(x_s)}. \quad (20)$$

Here, the phase shift is  $\delta_l(x_s) = \eta_l(x_s) + i\beta_l(x_s)$ , where  $\eta_l$  is the argument of the Jost function. In the present case (where absorption is present), the regular solution is defined by a boundary condition [Eq. (14)] which depends on  $x_s$ . This fact spoils many results of standard potential scattering theory. For example, for real  $x_s$

$$\varphi_l(x_s, x) \neq \varphi_l(-x_s, x),$$

$$f_l^{(+)}(x_s) \neq f_l^{(-)*}(x_s).$$

This last inequality shows that the S matrix is not unitary, i.e.,

$$S_l(x_s)^* \neq S_l(x_s)^{-1}.$$

As is easily seen from Eqs. (14) and (16), we shall have

$$g_l = \frac{l + \frac{1}{2}}{f_l^{(-)}(x_s)}. \quad (21)$$

Thus, the modulus of  $f_l^{(-)}(x_s)$  is related to the absorption probability via

$$1 - |S_l|^2 = \frac{x_s^2}{|f_l^{(-)}(x_s)|^2}. \quad (22)$$

In terms of the imaginary part of the phase shift the partial absorption cross section is

$$\sigma_l(x_s) = \frac{\pi}{x_s^2} (2l+1)(1 - e^{-4\beta_l(x_s)}). \quad (23)$$

### III. PARTIAL AND TOTAL ABSORPTION CROSS SECTIONS

In Figs. 1, 2, and 3 we plot our results for the imaginary part of the phase shifts ( $\beta_l$ ), the partial absorption cross sections ( $\sigma_l$ ), and the total absorption cross section ( $\sigma_A$ ) as functions of  $x_s$ , for different values of angular momentum  $l$ . All cross sections are expressed in units of  $r_s^2$ . These absorption parameters have been calculated from the exact radial solutions  $\varphi_l$ ,  $\mathcal{F}_{l(+)}$ , and  $\mathcal{F}_{l(-)}$  via the Jost functions given by Eq. (17). The power series expansions for the Jost and regular solutions given by Eqs. (11) and (9) are convergent in disjoint regions of the  $x$  plane. Because of this problem we have analytically continued both power-series expansions away from their convergence circles. (See the Appendix for details.)

For all values of  $l$  we find that  $\beta_l(x_s)$  is a monotonically increasing function of  $x_s$ , as one could expect from the shape of the effective potential (Fig. 6).

All  $\beta_l(x_s)$  are zero at  $x_s = 0$  and tend to infinity linearly with  $x_s$  as  $x_s$  increases to infinity. It follows from our results, that for low frequencies ( $x_s \ll 1$ ) the imaginary part of the phase shifts behaves as

$$\beta_l(x_s) = C_l x_s^{2l+2}. \quad (24)$$

Here, we found for  $C_l$  values in agreement with Starobinsky's formulas,<sup>4</sup> for  $x_s = 0$  and  $l = 0$ . However, the Starobinsky approximation is accurate only in a small neighborhood of  $x_s = 0$ . For example, the ratio

$$\frac{\beta_0^{\text{exact}}(x_s) - C_0 x_s^2}{\beta_0^{\text{exact}}(x_s)} \quad (25)$$

varies between 0.15 and 0.5 for  $0.05 \leq x_s \leq 0.1$ . For  $l = 1$ , the ratio (25) varies between 0.18 and 0.6 for  $0.05 \leq x_s \leq 0.1$ . That is, the inaccuracy of Starobinsky's approximation increases with  $l$  for fixed

small  $x_s$ .

Formula (24) can be derived from the low-frequency limit of the exact radial solution given by Persides.<sup>8</sup> In this limit, the radial solutions can be expressed in a closed form in terms of Legendre's functions  $P_l(x)$  and  $Q_l(x)$ :

$$\varphi_l(x, x_s) \underset{x_s \rightarrow 0}{\sim} (-1)^l P_l\left(1 - \frac{2x}{x_s}\right),$$

$$R_l(x, x_s) \underset{x_s \rightarrow 0}{\sim} \frac{i(-1)^l (2l)! (2l+1)!}{2^{l+1} (l!)^3 (x_s)^{l+1}} Q_l\left(1 - \frac{2x}{x_s}\right).$$

It follows from Eq. (17) that

$$f_l^{(-)} \underset{x_s \rightarrow 0}{\sim} \frac{(2l)! (2l+1)!}{2^{l+1} (l!)^3 (x_s)^l}. \quad (26)$$

From Eqs. (23) and (26), we obtain formula (24) with

$$C_l = \frac{2^{2l} (l!)^6}{[(2l)!]^2 [(2l+1)!]^2}.$$

The presence of a pole at  $x_s = 0$  for  $l \geq 1$  in the Jost function means that waves with very small frequency and nonzero angular momentum are repelled out of the vicinity of the black hole. For large values of  $x_s$  we find a good agreement between our exact results and the asymptotic formulas  $[\beta_l^{\text{as}}(x_s)]$  derived in Ref. 6, namely

$$\begin{aligned} \beta_l(x_s) &= \beta_l^{\text{as}}(x_s) + O\left(\frac{l + \frac{1}{2}}{x_s^{3/2}}\right) \text{ for } x_s \gg 1, \\ \beta_l^{\text{as}}(x_s) &= \pi x_s - \frac{1}{4} \ln 2 - \frac{1}{16} \left(\frac{\pi}{x_s}\right)^{1/2} - \frac{\pi}{2\sqrt{2}} \frac{(l + \frac{1}{2})^2}{x_s}. \end{aligned}$$

For example

$$\beta_0(2) = 5.79, \quad \beta_0^{\text{as}}(2) = 5.89,$$

$$\beta_1(2) = 4.98, \quad \beta_1^{\text{as}}(2) = 4.78.$$

We shall now consider the partial absorption cross-section  $[\sigma_l(x_s)]$  behavior. At  $x_s = 0$ , all  $\sigma_l(x_s)$  are zero except for  $l = 0$ . For the S wave,  $\sigma_0 = 4\pi$ .

This zero-frequency behavior is directly related to the presence of the singularity at  $x_s = 0$  in the Jost function [Eq. (26)] for  $l \neq 0$ . We find that for all  $l \geq 1$   $\sigma_l$  and  $\beta_l$  are practically zero in an interval  $0 \leq x_s \leq x_s^{(0)}(l)$  with  $x_s^{(0)}(l) \ll V_{\text{eff}}(\text{max})$  (see Table I), and also that  $\sigma_l(x_s)$  has a pronounced peak in the interval  $x_s^{(0)}(l) \leq x_s \leq x_s^{(1)}(l)$ . One finds that  $(x_s^{(1)})^2 \gg V_{\text{eff}}(\text{max})$  and that the absolute maxima of  $\sigma_l$  lie at a point  $x_s^M(l)$  of order  $[V_{\text{eff}}(\text{max})]^{1/2}$ . For  $x_s > x_s^{(1)}$ ,  $\sigma_l$  decreases monotonically with  $x_s$  as  $\sigma_l \simeq (2l+1)\pi/x_s^2$  because  $e^{-4\beta_l} \ll 1$  in this region [see Eq. (23)].

The values of  $x_s^M$  are given in a good approximation by geometrical optics. In this limit,  $x_s^M$  corresponds to the critical impact parameter<sup>9</sup>

TABLE I. Maxima of the partial absorption cross sections ( $\sigma_l^M$ ) for several partial waves. We give also the maxima of the effective potential [Eq. (8)] and the values of  $x_s^{(0)}(l)$  (see Sec. III for explanation).

$l$	$\sigma_l^M$	$x_s^{(M)}(l)$	$V_{\text{eff}}(\text{max.})$	$x_s^{(0)}(l)$
0	26.512	0.24	0.105	0
1	16.235	0.69	0.397	0.03
2	11.488	1.07	0.988	0.40
3	8.914	1.45	1.877	0.60
4	7.297	1.83	3.062	1.05
5	6.182	2.21	4.543	1.85
6	4.955	2.58	6.321	2.25
7	4.744	2.96	8.395	2.65

$$x_s^M = \frac{3\sqrt{3}}{2} (l + \frac{1}{2}) \simeq 0.38(l + \frac{1}{2}), \quad (27)$$

in good agreement with our results (see Table I). It follows from our results (Fig. 2) that the peaks of  $\sigma_l(x_s)$  are less pronounced for increasing angular momentum. For fixed frequency, the partial absorption cross section  $\sigma_l$  increases linearly with  $l$ , up to  $l \simeq (3\sqrt{3}/2)x_s$ , then it falls rapidly to zero.

This is related to the fact that the number of partial waves that contributes appreciably to the total absorption cross section ( $\sigma_A$ ) increases with the energy. This number is given approximately by  $(3\sqrt{3}/2)x_s$ . The behavior of the differential absorption cross section per unit solid angle  $d\Omega$  can be easily inferred for high frequencies from its partial-wave expansion

$$\frac{d\sigma_A(\theta)}{d\Omega} = \left| \sum_{l=0}^{\infty} (2l+1) g_l(x_s) P_l(\cos\theta) \right|^2, \quad (28)$$

and the properties of  $g_l(x_s)$ . For  $x_s \gg 1$ ,  $\sigma_A(\theta)$  will be peaked in the forward direction as follows from an approximate evaluation of series (28) for small angle, in terms of the Bessel function  $J_1$ ,

$$\frac{d\sigma_A(\theta)}{d\Omega} \underset{\theta \ll 1}{\underset{x_s \gg 1}{\simeq}} \frac{27}{4} \frac{x_s^2}{\theta^2} J_1\left(\frac{\sqrt{27}}{2} x_s \theta\right)^2.$$

Summing up the contribution of all significant partial waves we obtain the total absorption cross section ( $\sigma_A$ ) (Fig. 3) as a function of the energy. It presents an oscillatory behavior characteristic of a diffraction pattern, which can be interpreted as a consequence of the superposition of the peaks of each  $\sigma_l$ . The absolute maximum of each partial wave cross section produces a relative maximum in  $\sigma_A$ . Thus these relative maxima follow a law similar to Eq. (27). As frequency increases,  $\sigma_A$  oscillates around its constant geometric limit ( $\frac{27}{4}\pi$ ) with decreasing amplitude and approximately constant period ( $\simeq 0.38$ ).

We turn now to the physical interpretation of these results. As we have shown in a previous paper,<sup>7</sup> absorption may be interpreted as taking place only at the singularity ( $r=0$ ) of the Schwarzschild space. On the other hand, for large values of  $x_s$ , one can expect that Fresnel-Kirchoff diffraction theory will be applicable to our problem. Thus the absorbed radiation is given by the rays of the incident plane wave which arrive at  $r=0$ . The different rays will arrive by different paths, i.e., with different phases, and interference phenomena will take place. We interpret that this interference produces the oscillatory behavior of  $\sigma_A$ .

We shall now formulate a simple model which presents an absorption cross section qualitatively similar to a Schwarzschild black hole. We suppose that all ray paths are straight outside a sphere of radius  $R$ , but that rays fall radially inward for  $r < R$ . Of course, this is only a rough model for a black hole because the curvature of rays in the vicinity of the horizon has been neglected. The absorption cross section in this model will be proportional to the square modulus of the wave amplitude  $\Psi$  at the center of the sphere. In the Kirchoff-Fresnel approximation,<sup>12</sup> one has

$$\sigma_A \propto |\Psi|^2 = a \left| \int ds e^{ikR(1-\cos\theta)} \frac{1+\cos\theta}{2} \right|^2.$$

Performing this integration ( $ds$  stands for the surface element of the sphere), one finds

$$\sigma_A(kR) = \frac{R^2}{\pi} \left[ 1 - \frac{\sin 2kR}{kR} + \left( \frac{\sin kR}{kR} \right)^2 \right], \quad (29)$$

where we have chosen the constant  $a$  in such a way that  $\sigma(\infty) = R^2/\pi$ . Formula (29) describes qualitatively the total absorption cross section for a Schwarzschild black hole with

$$R = \frac{3\sqrt{3}}{2} \pi r_s.$$

An improved function that fits accurately the exact values of  $\sigma_A(x_s)$  is given by

$$\sigma_A(x_s) = \frac{27}{4} \pi - \frac{A}{x_s} \sin \pi \sqrt{27} (x_s + B). \quad (30)$$

The best fit is obtained for

$$A = 1.41 \sim \sqrt{2},$$

$$B < 10^{-4}.$$

In Fig. 4, we have plotted the total absorption cross section corresponding to an ordinary material sphere with a complex refractive index. It is a monotonically increasing function of frequency. Comparison with the oscillatory black-hole cross section shows clearly the differences between the absorption by a black hole and the absorption de-

scribed by complex potentials (optical models). For a black hole, the effective potential that describes the wave-black-hole interaction is real, but it is not Hermitian because of its singularity at the origin.<sup>7</sup> The presence of a nonzero absorption cross section is related to this non-Hermitian character.

#### IV. HAWKING EMISSION

In the context of classical field theory, the massless field  $\Psi$  obeying the wave equation (7) satisfies boundary conditions (14) guaranteeing that only absorption takes place. However, if quantum effects associated with the field  $\Psi$  are considered, the particle emission probability is nonzero and the spectrum of the emitted radiation is Planckian<sup>1</sup> [Eq. (1)]. By using the absorption cross section discussed in the preceding section we have calculated the Hawking emission for a wide range of frequency and angular momentum.

In Fig. 5 we plot the total emission spectrum as a function of  $x_s$ . We see that it does not show any

of the interference oscillations characteristic of the total absorption cross section (Fig. 3). This is related to the fact that the S-wave contribution predominates in Hawking radiation. The rapid decrease of the Planck factor for  $x_s \gtrsim 1$  suppresses the contribution of the partial waves with  $l \gg 1$ . For example, the maxima of  $H_l(k)$  for  $l=0, 1$ , and 2 are in the ratio  $1: \frac{1}{11} : \frac{1}{453}$ .

For angular momenta higher than two,  $H_l(k)$  is extremely small. The spectrum of total emission has only one peak following closely the S-wave absorption-cross-section behavior. Its maximum lies at the same point as the  $\sigma_0$  one ( $x_s^M = 0.23$ ).

The peaks of  $\sigma_1$  and  $\sigma_2$  turn out to have no influence in  $H(k)$ . In conclusion, Hawking emission is only important in the frequency range  $0 \leq k \lesssim 1/r_s$ .

#### ACKNOWLEDGMENTS

We wish to thank Brandon Carter for his valuable advice and encouragement. We thank Silvano Bonazzola for helpful discussions and his interest in this work.

#### APPENDIX

In order to perform the analytic continuation of the radial solutions  $\varphi_l(x, x_s)$  we seek power-series expansions for them in the neighborhood of an arbitrary point  $x = b$ . We write for a radial solution

$$R(x) = e^{-ix_s \ln|x-x_s|} \sum_{n=0}^{\infty} C_n (x-b)^n. \quad (A1)$$

By replacing (A1) in the radial differential equation (7) one obtains

$$\begin{aligned} b y^2 (n+1)(n+2) C_{n+2} + y(n+1) [y(n+1) + b(2n+1 - 2ix_s)] C_{n+1} \\ + \{ (b+2y)n^2 + [y - 2ix_s(y+b)]n + b(b^2 - x_s^2) - y(l+ix_s) \} C_n \\ + [(n-1)(n-2ix_s) + 3b^2 - l - x_s(i+x_s)] C_{n-1} + 3bC_{n-2} + C_{n-3} = 0, \end{aligned} \quad (A2)$$

where  $y = b - x_s$ . This recurrence relation defines all the  $C_n$ 's with  $n \geq 2$  in terms of  $C_0$  and  $C_1$ , i.e., the radial function and its derivative at  $r = b$ . For the regular solution  $\varphi_l(x, x_s)$  the analytic continuation is made as follows:

First, from the power-series expansion for  $\varphi_l$  we obtain  $\varphi_l$  and  $\varphi'_l$  at  $x = x_1$ , where  $x_1$  is near the extremum of the convergence interval ( $0 < x < 2x_s$ ). Then, by using the recurrence relation (A2) we calculate the coefficients of the series expansion for  $\varphi_l$  that converges in an extended interval

$$0 < x < 2x_1 \lesssim 4x_s.$$

This procedure is repeated iteratively. For the Jost solutions, a similar procedure is used to continue the function  $\mathcal{F}_{l(\pm)}(x, x_s)$  for low  $x$ .

<sup>1</sup>S. W. Hawking, Commun. Math. Phys. **43**, 199 (1975).

<sup>2</sup>B. Carter, Phys. Rev. Lett. **33**, 558 (1974).

<sup>3</sup>B. DeWitt, Phys. Rep. **19C**, 295 (1975).

<sup>4</sup>A. A. Starobinsky, Zh. Eksp. Teor. Fiz. **64**, 48 (1973) [Sov. Phys.—JETP **37**, 1 (1973)].

<sup>5</sup>D. N. Page, Phys. Rev. D **13**, 198 (1976).

<sup>6</sup>N. G. Sanchez, J. Math. Phys. **17**, 688 (1976).

<sup>7</sup>N. G. Sanchez, Phys. Rev. D **16**, 937 (1977).

<sup>8</sup>S. Persides, J. Math. Phys. **14**, 1017 (1973); Commun.

Math. Phys. **48**, 165 (1976); **50**, 229 (1976).

<sup>9</sup>C. W. Misner, K. S. Thorne, and J. A. Wheeler, *Gravitation* (Freeman, San Francisco, 1973).

<sup>10</sup>R. A. Matzner, J. Math. Phys. **9**, 163 (1968).

<sup>11</sup>R. G. Newton, *Scattering Theory of Waves and Particles* (McGraw-Hill, New York, 1966).

<sup>12</sup>M. Born and E. Wolf, *Principles of Optics* (Pergamon, New York, 1975).

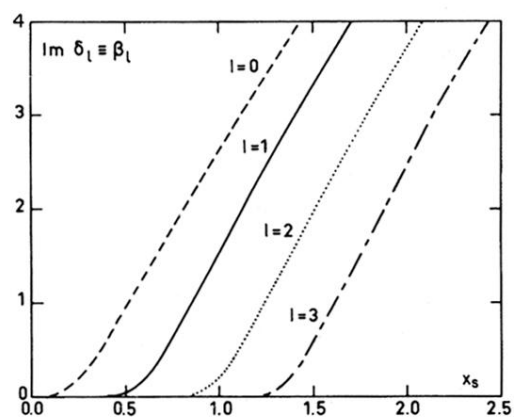


FIG. 1. Imaginary part of the phase shift for  $l=0, 1, 2, 3$ .



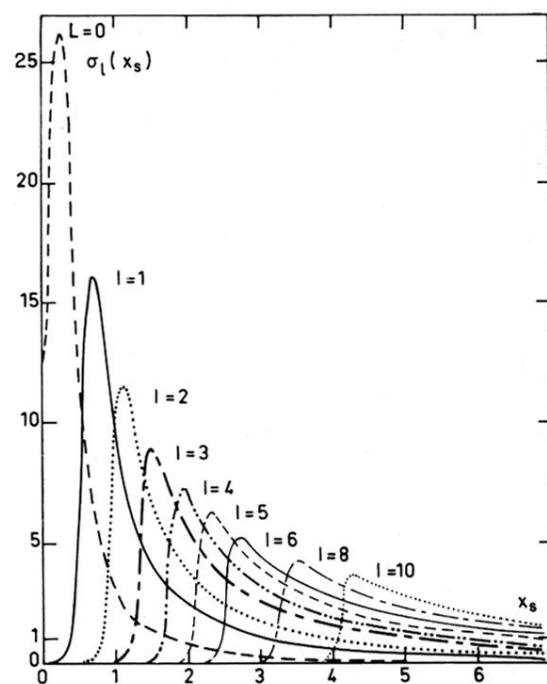


FIG. 2. Partial absorption cross sections  $\sigma_l(x_s)$  in units of  $r_s^2$ .

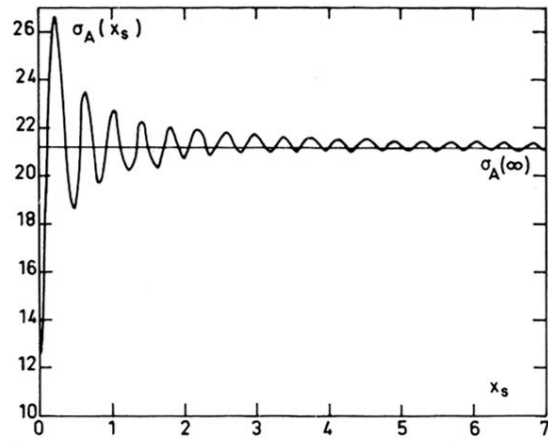


FIG. 3. Total absorption cross section  $\sigma_A(x_s)$  in units of  $r_s^2$  for a Schwarzschild black hole.

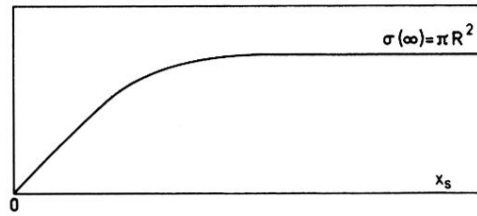


FIG. 4. Total absorption cross section for a material sphere with a complex refraction index. It can be noted that this absorption cross section attains its geometrical-optics limit ( $\pi R^2$ ) without any oscillations.

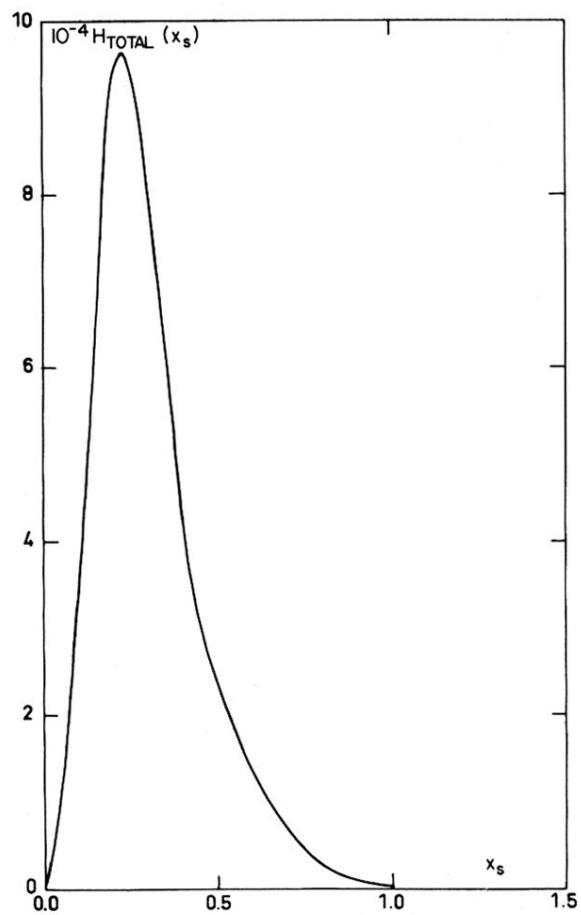


FIG. 5. Total emission spectrum for a black hole in units of  $1/r_s^2$ .

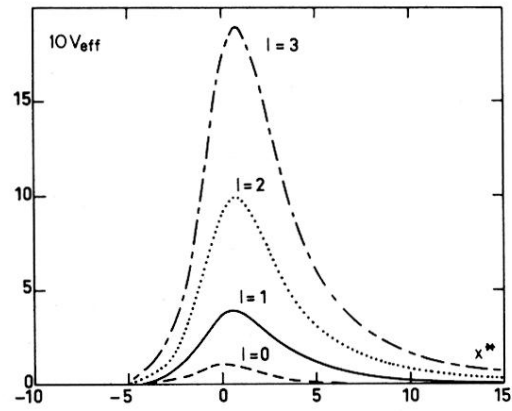


FIG. 6. Effective potential defined by Eq. (8) for  $l=0, 1, 2, 3$ .